An Integrated Approach to the Preliminary Weight Sizing of Small Electric Aircraft

C.E.D. Riboldi*[,a], F. Gualdoni[a]

[a]*Department of Aerospace Science and Technology, Politecnico di Milano, Milano, Via La Masa 34, 20156 Italy*

Abstract

Electric propulsion has received attention in aviation as witnessed by studies in hybrid designs and by the production of aircraft with support electric motors to be used in limited parts of the mission with ancillary roles. Until the recent past, the main limit to a wider adoption of electric propulsion, which besides having a lower environmental impact with respect to internal combustion engines (ICE) in terms of noise and emissions, can also improve reliability and on–board comfort, was the need for mass and volume–inefficient battery packs as devices for energy storage. However, thanks to the level of technology now reached by batteries, it is becoming possible to design and build electrically propelled aircraft at least in the category of light or general aviation. Due to the relative novelty of this technology, only few examples of similar aircraft exist today, mainly modifications of more traditional concepts, and thinking of a completely new electric aircraft is made difficult by the lack of a consolidated design framework, differently from the case of traditional ICE–powered models. This paper tries to cope with some basic aspects typical to electrically propelled aircraft, to the aim of setting up a stable and reliable preliminary sizing procedure allowing designers and aircraft companies to quickly size up and compare all–electric designs. To this aim, a statistical analysis of the basic characteristics of existing aircraft is presented first, showing a good correlation level between some of them. Next a method for the preliminary sizing of weights is shown, obtained starting from a more usual step–by–step procedure typically adopted for ICE–propelled aircraft. Due to the peculiar characteristics of electrically powered aircraft, the new procedure involves an integrated use of the case–specific mission profile and sizing matrix. The validity of the proposed procedure is testified by example analyses on two realistic designs of lightweight aircraft.

Key words:

electric aircraft, integrated design, preliminary weight sizing, optimal design

Nomenclature

AR	Aspect ratio

*Corresponding author, *Tel.:* +39-02-2399-8609; *Fax:* +39-02-2399-8334.

Email addresses: carlo.riboldi@polimi.it (C.E.D. Riboldi), federico.gualdoni@polimi.it (F. Gualdoni)

C_{bat}	Cost of batteries
C_{AC}	Purchase cost of aircraft
C_D	Drag coefficient
C_L	Lift coefficient
E_{bat}	Energy of batteries
E_{r}	Energy required (propulsive)
FAR	Federal Aviation Regulations
ICE	Internal Combustion Engine
J^{acro}	Merit function for acrobatic class
J^{tour}	Merit function for touristic class
K	Drag–due–to–lift polar coefficient
P_{bat}	Battery power
P_{m}	Power of electric motor
P_r	Power required (propulsive)
P_{SL}	Power required at sea level
R	Range of flight
RC	Rate of climb
S	Wing reference surface
SMP	Sizing Matrix Plot
T	Time of flight
TTC	Time to climb
W_{bat}	Battery weight
W_e	Empty weight
W_m	Motor weight

W_{pl}	Payload weight
W_{to}	Take–off weight
USD	United States Dollars
e	Battery–specific energy, Oswald coefficient
g	Gravitational acceleration
h	Altitude
p	Battery–specific power
q_C,q_R,q_{RC}	Optimization weights
γ	Climb angle
η_P	Propeller efficiency
λ	Energy–specific cost of batteries
ξ	Power loss coefficient
ρ	Density of air
τ	Power ratio

1. Introduction

Electric and hybrid propulsion systems have received a great deal of attention in recent years in various branches of transportation including aviation. This is due not only to the unpredictability of oil price in this era, making a less oil–dependent source of power more attractive for owners and operators in terms of cost and budget planning, but also to the better level of reliability and economy attained by electric motors [1, 2], as well as to the improved comfort generated by less noisy electric motors with respect to internal combustion engines (ICE) [3].

Nowadays, electric motors are generally more reliable than internal combustion engines (ICE), and their efficiency in converting stored energy into mechanical energy is much higher by constitution. The main limit to the usability of the electric alternative for propulsion has been bound to the limits of energy storage systems, i.e. batteries, which especially for aircraft did not offer until recently sufficient energy–to–mass and energy–to–volume densities [4] to be accommodated on board an aircraft without a relevant negative impact

on payload or aircraft size. Today, as a result of many research efforts towards the improvement of such performance indices, it is possible to design and fly an electrically propelled aircraft, as testified by some existing examples, both prototypical and production models, in the categories of ultra–light and general aviation [5].

Among the factors limiting the diffusion of the existing models of electric aircraft is their relatively high production cost, which will be only recursively lowered by the spreading of this technology, through know–how consolidation and scale economy effects. Also the cold perception by the potential customers plays a role in the lingering diffusion of such systems. Especially private pilots and flight training organization tend to be very cautious with respect to radically new technologies and prototype aircraft, when it comes to risking a relevant capital.

Also on the side of researchers and designers, the tendency to treat electric aircraft as prototypes is testified by the lack of literature illustrating a common framework for preliminarily designing such aircraft, which in most cases are obtained through a modification of existing machines, originally gliders or ICE–propelled designs. This is also due to some peculiar features of electric aircraft, requiring an analysis of the design point which will not be limited to those variables – basically empty and take–off weights, wing loading and power loading – usually considered for sizing a traditionally propelled aircraft. Some works exist in the literature about the similar issue of the sizing of hybrid propulsion aircraft [6, 7], but the futuristic assumptions concerning the performance of batteries and motors typically made in such analyses does not allow to consider these works for an immediate practical outcome. Some more realistic past research efforts are focused on parametric studies for all–electric designs, starting from a design point which is already well characterized, and from well proven data concerning the power–plant and the general sizing of the aircraft obtained from an existing testbed [8, 9]. Being based on precise measurements from an assigned aircraft example, these works do not present methods sufficiently general to allow application to a generic aircraft with given desired specifications. Another part of the literature on all–electric aircraft is devoted to the design and optimization of sub–systems on an assigned testbed, hence it is more centered on a later stage of the design, where the design point for the aircraft has been already determined [10]. Very little exists about the preliminary design of electric aircraft with respect to assigned mission requirements, trying to bend the procedures typically adopted for ICE–propelled aircraft to this new field of aeronautics. The lack of standard best practices among designers and aircraft builders in turn fuels the lack of confidence by customers, leaving the sector of electrically propelled aircraft in a condition of stagnation.

Trying to fill this lack in the existing literature, this script concentrates on the existing technology and introduces a possible simple way to preliminarily size electric aircraft, borrowing much from the preliminary design technique typically studied and implemented for ICE aircraft, but with some substantial modifications. A first fact that was noted is that the few electric aircraft already existing – both prototype and production

aircraft – clearly show a statistical correlation on some key design parameters. This fact, that will be suitably documented in the present paper, suggests a design approach starting from the statistical analysis of what has been done up to the present time. Subsequently, in the proposed sizing procedure, differently from the well–known procedures for non–electric aircraft where the analysis of the sizing matrix and the sizing of the aircraft weights are basically independent processes, these two areas of the design are intimately linked for the case of electric aircraft, due to the peculiar construction of the mission–specific correlation between weights for such design case. This yields and integrated procedure for sizing the new aircraft, where weights, wing loading and power loading influence each other, hence they need to be sized together.

In a first stage, the paper presents a statistical database of existing electric aircraft types and illustrates the sizing procedure at a theoretical level. In a subsequent section two examples of quantitative analyses are presented, showing the ability of the procedure to produce designs matching acceptable requirements typical to existing aircraft in the same weight class, thus proving its significance. In a final stage, it will be shown again through practical examples how the design method bends itself to an optimal analysis, thus making the potentially complex scenario of integrated design easier to deal with by means of a computationally–intensive approach. Finally, the approach and the results are recalled and critically discussed in the paragraph devoted to the conclusions.

2. Preliminary sizing of electric aircraft

2.1. Database of existing aircraft

Similarly to what is usually done for the preliminary sizing of ICE aircraft [11, 12], also for electric aircraft it is possible to set up a statistical analysis of the values assumed by some key parameters for some designs already existing. To this aim, in a first stage of the research the characteristics of some such aircraft have been collected and analyzed. The fact that an aircraft has been flown and the completeness of the available data on the electric plant have been considered as criteria for the inclusion of a model in the database.

Table 1 presents the values of some key construction parameters for the aircraft included in the database. For the sake of clarity, note that in this paper all weights are considered as a forces, hence they are measured in Newtons (N). When the corresponding masses are considered in plots or tables, they are properly referred to using the ratio W/g, where g is gravitational acceleration, as in Table 1. This expression for mass stems from the usual relationship between mass and weight force. Masses are expressed in kilograms (kg). Both mass and weight quantities are frequently used in aeronautics, sometimes with slight inaccuracies in their respective definitions. Here a distinction is made to preserve scientific rigor as much as possible.

The considered aircraft models fall in the category of general aviation or ultra–light aviation, whereas in terms of mission profile they are designed mostly for tourism and sporting activities (see Fig. 1).

#	Model	W_{to}/g[kg]	W_e/g[kg]	W_{bat}/g[kg]	W_m/g[kg]	Pm[kW]	e[Wh/kg]	p[W/kg]
1	ElectroLight 2 [13]	315	188	34	7.0	19.4	163.2	795.6
2	LAK–17B FES [14]	550	246	32	7.3	35.3	131.3	910.9
3	Lange Aviation Antares 20E [15]	660	440	77	29.1	42.0	136.0	794.0
4	Lange Aviation Antares 23E [15]	850	496	77	29.1	42.0	136.0	794.0
5	Pipistrel Taurus Electro G2 [16]	550	253	42	11.0	40.0	113.1	952.4
6	UAV Factory Penguin BE [17]	21.5	9.83	4.41	0.650	2.7	145.0	807.1
7	Yuneec International E430 [18]	470	157	74	19.0	40.0	153.7	801.0
8	Silent 2 [19]	300	200	36	8.5	13.0	113.9	792.4

Table 1: Database of electrically propelled aircraft already flying.

(a) Pipistrel Taurus Electro G2 [16]

(b) Yuneec International E430 [18]

Figure 1: Example aircraft in the database in Table 1.

Due to the particular nature of electric aircraft, it is necessary to introduce some analytical relationships between the various weights, which do not always have a counterpart in the design of ICE aircraft.

The take–off weight W_{to} and the empty weight W_e are related by the definition

$$W_{to} = W_e + W_{pl} + W_{\mathrm{bat}} + W_m \tag{1}$$

where W_{pl} is the weight of payload, W_{bat} the weight of batteries, and W_m the weight of the electric motor.

Other quantities relevant to the analysis reported in Table 1 are the energy density and power density of the batteries for each of the mentioned existing aircraft. These quantities are defined respectively as $e = \frac{E_{\mathrm{bat}} g}{W_{\mathrm{bat}}}$ and $p = \frac{P_{\mathrm{bat}} g}{W_{\mathrm{bat}}}$, where g is gravitational acceleration, E_{bat} the stored energy and P_{bat} the peak output power of the battery. These parameters are specific to the technology of the battery [5]. In this regard, it is noteworthy that the average value of the specific energy for the aircraft in the database is $e_{av,DB} = 139.75$ Wh/kg, with a small relative standard deviation of $\frac{\sigma(e_{DB})}{e_{av,DB}} = 11.6\%$. These values are typical to Li–ion batteries currently manufactured for general purpose applications, and $e_{av,DB}$ is much less than what is usually assumed in the literature when dealing with future designs [20, 21]. Information concerning futuristic values of energy–related quantities characterizing the batteries, thought to reach over three times the reported $e_{av,DB}$ by 2020, have not been considered relevant in this work, which is focused on realistic design of aircraft at the current technological level. Furthermore, the cost behind the technological effort needed to reach the predicted figure is hard to quantify, hence accounting for it would make further analyses less safe in terms of cost assessment.

From Table 1 it is apparent that the number of aircraft entries is not very high, and this is obviously a potential limit for the present analysis. On the other hand, from Fig. 2 it is possible to notice that the empty and take–off weights for all considered entries in the database fall in a limited range and are also well correlated. This highlights an existing relationship between W_e and W_{to} for aircraft in the considered weight category, which comes in the usual logarithmic form (see Part I of the book by Roskam [11])

$$\log(W_{to}) = A + B \log(W_e) \tag{2}$$

thus appearing linear on a logarithmic plot as in Fig. 2.

Other parameters for which a statistical correlation appears to exist are weight and power of the electric motors. In this case, the best match is with as semi–logarithmic curve, in the form

$$\log W_m = C + D P_m. \tag{3}$$

where P_m is the power of the electric motor.

Figure 3 shows the data and the correlation corresponding to Eq. 3 on a semi–logarithmic plane.

It can be noticed that the similarity between the values of installed power of most entries in the database does expose further analyses to the need to extrapolate for a motor weight or power higher than those

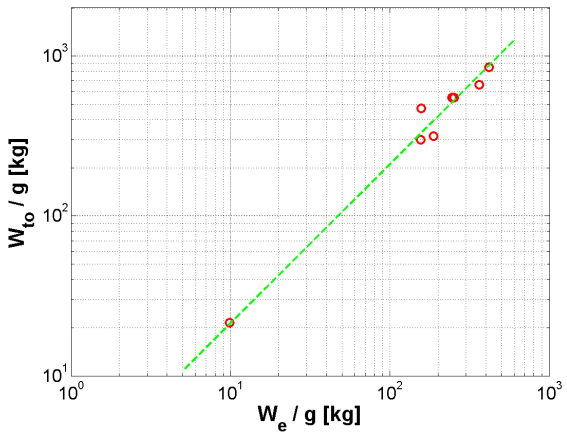

Figure 2: Take–off (W_{to}) vs. empty (W_e) weight. Original data and regression curve.

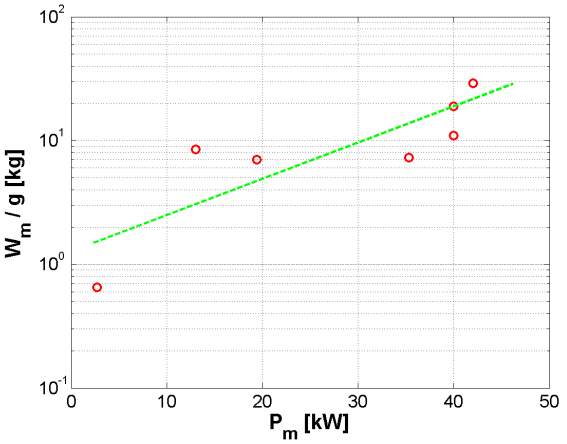

Figure 3: Motor weight (W_m) vs. power (P_m). Original data and regression curve.

considered. The correlation tends to diverge rapidly to unrealistic values of motor weight for power values slightly higher than those considered in the database. To avoid this, the correlation in Eq. 3 will be used only on the domain consisting of the values between minimum and maximum installed power in the database, whereas out of this domain another realistic relationship will be introduced later for sizing.

2.2. Integrated analysis of the mission profile and design constraints

In order to correctly exploit the data in Table 1, the present work is mainly focused on small aircraft, ideally for cross–country flight or training, thus matching the type of aircraft considered in the database. With this in mind, taking into account the typical mission of existing aircraft in the database, it was decided to consider in the mission profile five usual phases: take–off, climb, cruise, loiter and landing.

For ICE–propelled aircraft, the well–known sizing method by Raymer [12] (see Chapters 3 and 6) makes use of the definition of take–off weight as a function of fuel weight and empty weight plus payload, and tries to link the decrease of weight from take–off to landing to the flight mechanics parameters of each phase of the flight. To this aim the same method makes use of fuel fractions, i.e. ratios between the weight of the aircraft at the beginning and at the end of each phase of the flight. Fuel fractions are defined as analytical functions of range and endurance as well as other aerodynamic and engine–specific parameters for cruise and loiter respectively, or explicitly guessed for shorter phases like take–off and landing. By solving a 2–by–2 system between the regression of historical W_{to} vs. W_e data (Eq. 2) and the analytical relationship between the same quantities obtained from the mission profile, it is possible to find in a standard design scenario values for W_{to} and W_e representing a feasible design solution in terms of weights that also accomplishes the mission goals.

This procedure is clearly not applicable to the case of electric aircraft, due to the time–varying fuel weight being ideally substituted by the fixed battery weight in the definition of take–off weight (Eq. 1). Furthermore, the requirements for the various phases of the mission cannot be translated into the assignment of fuel fractions, which are themselves meaningless variables in the case of electric aircraft, when the weight of the aircraft is the same during all the mission.

In order to retain most of the approach used in the traditional non–electric design scenario, it is necessary to obtain a relationship between the weights in Eq. 1 and the mission requirements. In this section we show a possible way of computing the effect of some key mission parameters on the weights and especially on W_{bat}, passing through the definition of the amount of energy and power required for each phase of the flight.

2.2.1. Mission analysis through flight mechanics

Going back to the considered mission profile, the most prolonged phases of the flight are climb, cruise and loiter. The performance can be characterized for each of them by referring to basic static equilibrium equations from flight mechanics [22].

Concerning climb, a typical requirement can be defined in terms of a target constant rate of climb RC (see [11] Part I). The equilibrium equation in presence of a non–null vertical speed can be written as in Eq. 4

$$P_r^{\text{climb}} = W_{to} RC + \frac{1}{2}\rho^{\text{climb}} {V^{\text{climb}}}^3 S C_D^{\text{climb}} \tag{4}$$

where the average air density ρ^{climb} during climb, the constant airspeed V^{climb} and the value of the drag coefficient C_D^{climb} need to be known in order to compute the power required for climb P_r^{climb}.

Concerning the value of the drag coefficient, it can be estimated by firstly guessing the polar of the aircraft. In preliminary design where very little of the aircraft is known, the procedure proposed by Roskam can be applied for estimating the coefficients of the polar in the usual parabolic form $C_D = C_{D,0} + KC_L^2$ (see [11], Part I). The procedure calls for a guessed value of aspect ratio AR, which can be estimated from similar aircraft, and a possible level of refinement of the aerodynamic design, influencing the value of parasite drag $C_{D,0}$ through empirical correlation. Estimates for the values of $C_{D,0}$ and $K = \frac{1}{\pi \cdot AR \cdot e}$, where e is here the Oswald coefficient, can be corrected making use of the same method accounting also for flap deployment and extended landing gears, thus obtaining polars for various aircraft configurations, including clean, take–off and landing.

In the case of climb, cruise and loiter a same polar referring to a clean configuration can be assumed. Provided $C_{D,0}^{\text{clean}}$ and K^{clean} have been estimated somehow, it is possible to compute the value of the lift coefficient from vertical equilibrium for an assigned airspeed, as

$$C_L = \frac{2W_{to}}{\rho V^2 S} \tag{5}$$

thus yielding a value for C_D from the analytic polar of the aircraft in clean configuration.

Alternatively, once the polar is known, a given C_L can be imposed, theoretically capable of optimizing some performance index, like time–to–climb or distance–to–climb. In such case it is always possible to compute C_D from the analytic polar, using Eq. 5 to find the corresponding V for equilibrium, and finally feeding the equation for required power (e.g. Eq. 4 for climb) to find P_r for the considered phase.

It should be remarked that using the take–off weight W_{to} in Eq. 5 for every phase of the flight is not an approximation, differently from the case of ICE–propelled aircraft, due to the fact that this quantity is constant for the whole duration of the flight for electric aircraft. On the contrary, ρ^{climb} is representative of all altitudes crossed during climb, hence using this value brings in some approximation. However, for the considered class of aircraft, typically unpressurized and flying at relatively low levels, this approximation is still acceptable in this preliminary phase, provided a proper value is assumed for ρ^{climb}.

The energy required for the climb phase can be computed through an estimate of the time–to–climb TTC, which can be defined as

$$TTC = \frac{h^{\text{cruise}}}{RC} \tag{6}$$

where h_{cruise} is the cruising altitude. Therefore, the energy required for the climb phase can be obtained by definition as

$$E^{\text{climb}} = P_r^{\text{climb}} TTC \tag{7}$$

The cruise and loiter phases can be treated in a similar way to get the corresponding required energy and power values. For both cruise and loiter, the power required comes from static equilibrium in the longitudinal direction as

$$P_r = \frac{1}{2}\rho V^3 S C_D \tag{8}$$

where ρ, V, C_D and hence P_r will be typically different for the two considered flight phases. For cruise the usual requirements come in the form of an assigned airspeed V^{cruise} and range R. The resulting time for cruise will be

$$T^{\text{cruise}} = \frac{R}{V^{\text{cruise}}}. \tag{9}$$

It should be noted that differently from the climb phase, where an approximation was made in the computation of TTC assuming a single value of density ρ^{climb} for all altitudes during climb in Eq. 6, the definition of the value of T^{cruise} in Eq. 9 is exact. As weight does not change during the flight, differently from ICE–propelled aircraft, for electric aircraft the value of cruise speed can be maintained constant without power adjustments for all the duration of the cruise.

For a given V^{cruise}, using vertical equilibrium (Eq. 5) it is possible to obtain C_L^{cruise} and from the clean polar of the aircraft the value of C_D^{cruise}. The energy required for cruise is defined as

$$E^{\text{cruise}} = P_r^{\text{cruise}} T^{\text{cruise}}. \tag{10}$$

The loiter phase can be treated formally in the same way as cruise. As usually the loiter time T^{loiter} is part of the requirements, it is easy to compute the value of the energy required for this part of the flight as

$$E^{\text{loiter}} = P_r^{\text{loiter}} T^{\text{loiter}}. \tag{11}$$

From the computation of the required energy and power for the various phases of the flight it is possible to estimate the weight of the batteries and motor that need to be installed in order to allow flying the intended mission profile. In order to do so, values of energy density e and power density p need to be assumed. It is possible to set these quantities to realistic average values obtained from the database of existing aircraft. Batteries will be designed on the most stringent requirement among those bound to energy and power, whereas the weight of the motor will be sized using the statistical regression previously shown (Eq. 3) on the basis of the value of required power.

It should be observed that Eq. 4, 7, 8, 10 and 11 refer to energy and power required from the viewpoint of flight mechanics performance. In order to translate these desired performance figures into energy and power

requirements for the electric motor and batteries, it is necessary to account for the propulsive efficiency $\eta_P < 1$ of the propeller. This yields a higher requirement on batteries and motor than what is obtained from pure flight mechanics analyses.

In analytical terms, the value of battery weight from the mission profile $W_{\text{bat},MP}$ can be defined as

$$W_{\text{bat},MP} = \frac{g}{\eta_P} \max \left\{ \frac{E^{\text{climb}} + E^{\text{cruise}} + E^{\text{loiter}}}{e} \, , \, \frac{\max \left\{ P_r^{\text{climb}} \; P_r^{\text{cruise}} \; P_r^{\text{loiter}} \right\}}{p} \right\}. \tag{12}$$

Concerning the electric motor, the historical regression presented in Eq. 3 can be used. As previously stated, due to the peculiar shape of such regression curve, yielding extreme weight values for required power slightly above the top database entries, the following procedure has been adopted to cope with higher values of required power, based on the value of $P_r = \max \left\{ P_r^{\text{climb}} \; P_r^{\text{cruise}} \; P_r^{\text{loiter}} \right\}$:

$$\begin{aligned} \text{if } \left(\frac{P_r}{\eta_P} \right) \in [P_{\min,DB}, P_{\max,DB}] \; &: W_m = \exp \left(C + D \left(\frac{P_r}{\eta_P} \right) \right) \\ \text{if } \left(\frac{P_r}{\eta_P} \right) > P_{\max,DB} \; &: \tilde{W}_m = \exp \left(C + D P_{\max,DB} \right) \\ &\tau = \left(\frac{P_r}{\eta_P} \right) / P_{\max,DB} \\ &W_m = \tilde{W}_m \tau \end{aligned} \tag{13}$$

The procedure in Eq. 13 is of course arbitrary in its analytic form, but it tries to model the increase in W_m with P_r more realistically than with a simple extrapolation. The proposed procedure can be interpreted hypothesizing that an increase of required power over the maximum recorded in the database for a single engine can be coped with through a milder increase in weight, bound to power through a linear relationship instead of an exponential one. This is in accordance with the fact that over a certain amount of required power it is typical to increase the number of smaller engines instead of implementing an overloaded single one.

As previously pointed out, the proposed procedure allows to compute explicitly the values of the weights for the propulsion system, i.e. W_{bat} and W_m. The relationship between empty weight W_e and take–off weight W_{to} accounting for W_{bat} and W_m comes from the definition of take–off weight in Eq. 1. A very relevant difference with respect to ICE–propelled aircraft is that Eq. 1 for electric aircraft is explicit in both W_e and W_{to}, whereas according to the usual sizing procedure for ICE–propelled aircraft (see Chapter 3 in [12]) it should be possible to express W_{to} as a function of the ratio $\frac{W_e}{W_{to}}$, i.e. the product of the fuel fractions for each phase of the flight, in turn obtained from the analysis of the mission profile. In other words, the weight of fuel is not present explicitly in the solution of the design point in terms of weights for ICE–aircraft, whereas the weight of batteries is in the case of electric aircraft. Therefore, in the case of electric aircraft it is necessary to guess a value of W_{to} in order to compute W_e or viceversa from Eq. 1, and the difference between these values is due to W_{bat}, W_m, computed as illustrated above, and an assigned W_{pl}.

The take–off and landing phases have not been accounted for explicitly in the proposed analysis of the mission profile. This is due to their usually very low incidence with respect to the other phases of the flight in the sizing of battery weight. Such incidence has been investigated in this work with simplified but very conservative energetic models, and found to be responsible in any case for less than 1% of the total W_{bat}. Therefore, take–off and landing may be safely accounted for by simply increasing the value of W_{bat} computed based on the analysis of the other three phases by a factor of 1.02.

2.2.2. Design constraints from sizing matrix plot

Two further remarks concern the equations involved in the analysis of the mission profile. Firstly, Eq. 5, which is instrumental in computing the power required for the various phases of the mission profile, depends on wing loading $\frac{W_{to}}{S}$. Secondarily, the equations for required power (Eq. 4 and 8) depend explicitly on the reference surface S, but they can also be rewritten as relationships between power loading $\frac{W_{to}}{P}$ and wing loading $\frac{W_{to}}{S}$.

Similarly to the case of ICE–propelled aircraft, the explicit solution of the design point in terms of W_e and W_{to} can be obtained by solving the system constituted by the historical regression Eq. 2 and the definition of weight Eq. 1. Differently from ICE–propelled aircraft, wing loading $\frac{W_{to}}{S}$ must be specified in order to complete the computation of weight using the mission equations typical to the mission profile. In the conventional scenario of ICE–propelled aircraft a target value for the wing loading can be defined together with power loading $\frac{W_{to}}{P}$ based on the analysis of the sizing matrix. The target power loading is defined by constraints pertaining both to typical maneuvers encountered during the mission, including those considered in the mission profile, and to regulations (i.e. certification constraints).

Due to the fact that wing loading is a significant parameter for both the sizing matrix analysis and for the weight estimation procedure described above, which is typical to electric aircraft, it makes sense to consider an integrated sizing approach where the value of the wing loading specified in order to comply with sizing matrix constraints is used as a constraint for the explicit computation of the design weight. Once the wing loading has been defined, for a given take–off weight W_{to} it is possible to obtain the corresponding reference surface S, so that the computation of power and hence of energy required for the mission profile can be carried out explicitly, following the procedure presented in the previous sub–section, leading to an estimation of all weights. The result of the weight sizing procedure will be implicitly compliant with respect to the constraints expressed in terms of power loading and wing loading from the analysis of the sizing matrix.

The analysis of the sizing matrix can be setup considering the potential certification framework for the aircraft of interest here. Once again, it is possible to refer to the database to see that a potential certification class for the aircraft in it is that of general aviation aircraft. Therefore, FAR Part 23 rules can be used as guidelines to setup the equations of the sizing matrix.

Seven constraints should be considered, namely take–off, landing, climb in take–off and landing configuration, climb at a specified speed and rate of climb (from the mission profile), cruise and loiter. The analytic expressions of such constraints are the same for electric aircraft and conventional aircraft, hence they can be found in the literature [11] (see Part I) for those coming from certification procedures, or by manipulation of Eq. 4, 5, 8 for those coming from the mission profile. The curves corresponding to each constraint can be plot on the plane $\frac{W_{to}}{P}$ vs. $\frac{W_{to}}{S}$ (sizing matrix plot, SMP, see [12] Chapter 19 and [11] Part I).

Some requirements for the aircraft need to be guessed in order to set some parameters in the equations of the constraints coming from regulations as well as from the mission profile. For take–off, the ground run distance needs to be assigned. For climb in take–off and landing configurations the respective polars of the aircraft must be assigned, and they can be obtained at this stage using the procedure proposed by Roskam and already mentioned above for obtaining $C_{D,0}^{\text{clean}}$ and K^{clean}. For the constraint represented by cruise speed, it is necessary to know V^{cruise}. For the constraints coming from the mission profile, the clean polar, climb, cruise and loiter speeds, and the vertical speed RC during climb need to be assigned. Furthermore, altitudes for all maneuvers need to be guessed.

Figure 4 presents a possible SMP for a prototype mission for which the constraints have been specified based on the investigation of the characteristics of the aircraft in the database. In particular, the take–off ground run distance has been set to 200 m at sea level, and cruising and loiter altitude has been set to 1500 m. Polar coefficients have been obtained imposing an $AR = 30$ and a certain level of cleanliness of the aerodynamic construction, that is typical to gliders or lightly powered aircraft. Furthermore, no retractable landing gear have been hypothesized, and no deployment of flaps on take–off, that is typical to smaller aircraft. For landing, stall speed has been set to $V_{\text{stall}}^{\text{landing}} = 40$ kn (= 20.4 m/s) at sea level. Some curves in Fig. 4 are parameterized, in particular for different values of $C_{L,\max}$ for the landing constraint and for various C_L^{to} for take–off. Climb, cruise and loiter speeds $V^{\text{climb}} = 48$ kn (= 24.7 m/s), $V^{\text{cruise}} = 90$ kn (= 46.3 m/s) and $V^{\text{loiter}} = 81$ kn (= 41.7 m/s) respectively are assigned for the corresponding phases. Further quantities assigned are the vertical speed in climb in clean configuration, $RC = 400$ ft/min (= 2.02 m/s) and the average density during climb.

The curves representing the constraints on the sizing matrix plot define an area of compliance with respect to all constraints. With the information available at this stage, a possible rule for choosing a design point on the SMP is that of maximizing wing loading, thus reducing the size of the reference surface, and hence of the aircraft, for a given W_{to}. Secondarily, it is possible to set power loading to the highest possible value, in order to assure the lowest power required with respect to a same take–off weight, hence reducing motor weight and cost.

The values of $\frac{W_{to}}{P}$ and $\frac{W_{to}}{S}$ for all aircraft in the database have been reported on the plot in Fig. 4, showing that all aircraft fall in the space of solutions defined by the adopted constraints. A propulsive

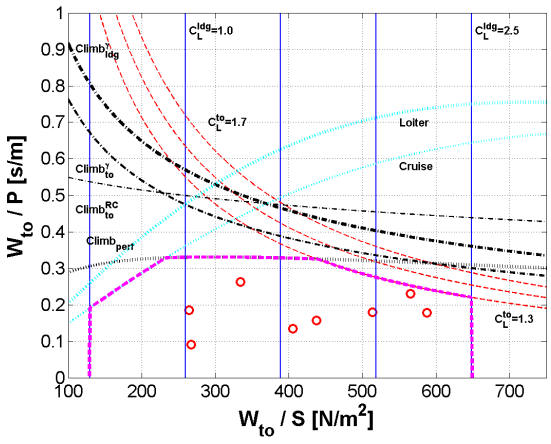

Figure 4: Sizing matrix plot (SMP) and historical data. Blue solid vertical lines: landing for various C_L values. Red dashed lines: take–off run for various choices of C_L^{to}. Black dash–dotted lines: climb (two in take–off configuration with assigned climb angle γ and rate RC, one in landing configuration with assigned angle γ as specified by FAR Part 23). Black dotted line: climb with assigned speed and rate RC from mission profile. Cyan dotted lines: cruise and loiter. Magenta dashed line: envelope. Red circles: historical data.

efficiency $\eta_P = 0.86$ has been hypothesized for all database aircraft. Some of those aircraft are actually far from the borders of the space. This only means that the numerical specifications used for the plot of the constraints are less demanding than those considered for the actual design of some of the considered aircraft.

A more thorough study of the SMP will be presented through some examples in the section devoted to the results.

2.2.3. Selection of the design point through integrated analysis

As explained above, in order to close the problem of finding W_{to} and W_e it is possible to specify a value of $\frac{W_{to}}{S}$, providing a way to explicitly write the equations for the mission profile and computing W_{bat}. Such value can be obtained from the analysis of the SMP, so that all constraints on the plot be implicitly satisfied in terms of wing loading. In practice, the assigned value of wing loading can be used to find the value of the reference wing area $S = W_{to} / \left(\frac{W_{to}}{S}\right)$, thus allowing to compute W_e for a given W_{to} through the power equations of the mission profile.

Similarly, a value of power loading $\frac{W_{to}}{P}$ can be obtained from the analysis of the SMP that satisfies all constraints from the mission profile and from regulation or required standard maneuvers. From the viewpoint of the procedure presented above for sizing W_{bat}, the power loading information coming from the analysis of the SMP may be included as a constraint to the maximization written in Eq. 12, which consequently can be

extended yielding

$$W_{\text{bat}} = \frac{g}{\eta_P} \max \left\{ \frac{E^{\text{climb}} + E^{\text{cruise}} + E^{\text{loiter}}}{e} , \frac{\max \left\{ P_r^{\text{climb}} \; P_r^{\text{cruise}} \; P_r^{\text{loiter}} \; W_{to} / \left(\frac{W_{to}}{P} \right) \right\}}{p} \right\} \tag{14}$$

where the latter term $W_{to} / \left(\frac{W_{to}}{P} \right)$ brings the level of power loading chosen to satisfy all constraint on the SMP as a constraint in the computation of necessary power from the mission profile. It is clear from Eq. 14 that in case the top required power is due to the requirements coming from the mission profile there will be no numerical difference between this maximum power and that computed in the previous Eq. 12. In any case, the power requirement has still to be compared with the energy requirement in order to check what is the governing value in the computation of W_{bat}.

The work–flow diagram in Fig. 5 summarizes how the integrated procedure for preliminary sizing shown in this section can be setup.

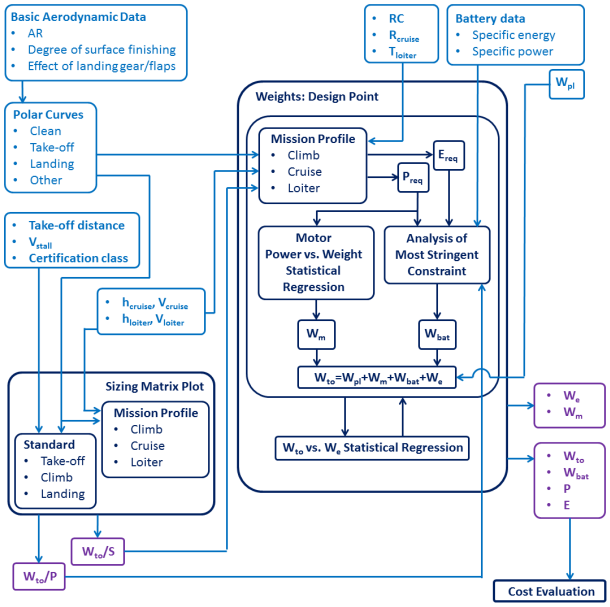

Figure 5: Work–flow of integrated preliminary sizing procedure.

In particular, it should be noticed that there are two main operational blocks (in dark blue in the figure), one representing the sizing matrix plot and producing design wing loading and power loading values, the other representing the explicit weight sizing procedure, resulting in design values for all weights in Eq. 1. The equations for the mission profile are present in both main blocks, providing constraints on the SMP and on one of the sub–procedures in the weight sizing block. The latter is centered on assembling the general definition of weights for an electric aircraft (Eq. 1), which is possible computing the battery weight and motor weight from the requirements of the mission profile. A 2–by–2 system in the unknowns W_{to} and W_e is setup

next, composed of the weight definition (Eq. 1) and of the historical regression of W_{to} and W_e data from the database (Eq. 2).

3. Quality of the design point

The choice of the design point is often the result of a parameterized analysis, intended also to assess the sensibility of a possible design solution with respect to changes to the mission requirements and constraints. From the computational viewpoint, the design point is obtained having the requirements as basic input. Thus altering the requirements causes the need to re–run the design procedure correspondingly. Luckily, the procedure presented above is based on light computations, which can be performed in multiple instances in a short time on an average processor. For this reason, the design procedure presented above bends itself to a parameterized analysis.

In order to better assess the effect of some design parameters on quantities not directly related to flight mechanics, yet interesting for the design, a possible performance index to be considered is cost. This can be split into aircraft and battery cost.

A basic model for the manufacturing cost of small aircraft is constituted by a linear–quadratic function of the take–off weight alone W_{to} [23]. For the aircraft in the database this model may be not highly accurate, due to its partly experimental nature. Nonetheless, the values obtained are comparable with those obtained for other ICE–propelled aircraft of the same size and level of complexity [24]. The equation for the aircraft cost yields

$$C_{AC} = 4.649 \cdot 10^{1} W_{to} + 2.85 \cdot 10^{-2} W_{to}^{2} \tag{15}$$

with W_{to} in N and the cost C_{AC} in USD. Similarly to the case of ICE–propelled aircraft, C_{AC} does not include fuel – and hence battery – cost.

Concerning the cost of batteries, several statistical relationships can be found in the literature bearing somewhat scattered results depending on the considered database [5, 23, 27, 28, 29]. In this work, reasonable results have been obtained using the data of an analysis by Kromer and Heywood on Li–ion batteries employed on hybrid vehicles [5]. This analysis links the specific cost of batteries λ in USD/(Wh) to the ratio of power–to–energy of the battery, $\frac{P_{\text{bat}}}{E_{\text{bat}}}$ in 1/s. The latter can be computed in the procedure proposed in the present work at the level of the mission profile analysis, after having estimated the required energy and power for the whole mission. The correlation between $\frac{P_{\text{bat}}}{E_{\text{bat}}}$ and λ can be obtained based on a linear regression on the data proposed by Kromer and Heywood, such that $\lambda = M + N\frac{P_{\text{bat}}}{E_{\text{bat}}}$. In this expression the coefficients are $M = 0.2362$ USD/(Wh) and $N = 0.0138$ USD/W, whereas the average absolute normalized error between the data and the linear correlation is 1.76% – a very low value, raising confidence in the adopted linear regression

function. Therefore, an expression for the cost of batteries C_{bat} in USD can be written as

$$C_{\text{bat}} = e\lambda W_{\text{bat}}/g. \tag{16}$$

As shown on the work–flow diagram in Fig. 5 the evaluation of aircraft and battery cost can be completed aside from the main computations, after the weights necessary for running the cost model have been found.

A possible way to set up a parametric analysis is constituted by simultaneously studying more measures of performance, wrapped together in a merit function. The value of this measure of merit can be mapped with respect to parameters relevant to the design, having an impact on the selected measures of performance. Furthermore, provided the merit function features a suitable dependence on its parameters, it is possible to seek for its optimum. This will correspond to a stationary condition of the merit function, obtained with particular, optimal values of the parameters. If the parameters considered in the analysis can be considered as tunable variables, i.e. they are not fixed and can be governed by the designer, it is possible to exploit the information obtained from the map of the merit function to select an optimal design condition, corresponding to optimal values of the parameters. Such criterion of optimality is often adopted for the choice of the design point.

The approach to parametric analysis just described will be applied to the case of two example designs by first building–up suitable merit functions. Flight mechanics quantities that are usually interesting to maximize for an aircraft in the touristic category are those related to the cruise and loiter phases, in particular range. An increase in this performance index usually comes together with an increased take–off weight. Cost is a measure that penalizes an increase in weight, specifically W_{to} and W_{bat} in the models just introduced (Eq. 15 and 16). In order to help defining a design point in the space of the possible solutions, it is possible to setup an optimality problem based on a merit function J^{tour} including both range and cost, or analytically

$$J^{\text{tour}}(W_{to}, R) = q_C \left(C_{AC} + C_{\text{bat}}\right) - q_R R \tag{17}$$

where q_C and q_R are weights of cost and range respectively.

This means that if a change in the range requirement is acceptable, this new degree of freedom in the sizing problem can be used to steer the design point in order to obtain the maximum of J^{tour}.

Similarly, for aircraft for which maneuvering performance is more relevant than range, vertical speed can be used instead of range to form a merit function J^{acro} together with aircraft cost. Hence for an acrobatic aircraft

$$J^{\text{acro}}(W_{to}, RC) = q_C \left(C_{AC} + C_{\text{bat}}\right) - q_{RC} RC. \tag{18}$$

where q_C and q_{RC} are weights of cost and rate of climb respectively.

In this case RC will represent a new degree of freedom in the problem, i.e. a tunable design requirement.

For both considered cases an optimal problem can be posed as the minimization of the respective J subject to some constraints, or analytically

$$\min_{\boldsymbol{p}} J \text{ s.t. : } \begin{cases} \text{Certification requirements} \\ \text{Standard maneuvers (take–off, landing)} \\ \text{Mission profile} \\ W_{to} \text{ vs. } W_e \text{ regression of historical data} \end{cases} \tag{19}$$

where in case $J = J^{\text{tour}}$ then the array of optimization parameters is $\boldsymbol{p} = \{W_{to}, R\}$, whereas in case $J = J^{\text{acro}}$ then $\boldsymbol{p} = \{W_{to}, RC\}$.

In Eq. 19 the first three constraints have an effect at the level of the SMP, which translate into a choice of wing and power loading. The equations of the mission profile are further used together with the historical regression W_{to} vs. W_e to compute the value of all weights including W_{to}, other flight mechanics parameters and cost which appear in the merit function J.

It should be remarked that various other performance parameters could be included in the merit function as well, like for instance the cruising speed. The choice of the variables of interest is bound to the intended mission and specific design requirements. Furthermore, more degrees of freedom might be freed up together, making the optimal analysis more comprehensive, but less intuitive. In the results section some hints will be presented about possible optimal analyses, with an accent on studying the behavior of the respective merit functions instead of concentrating on the search of the optimum – which thanks to the regularity and the size of the problem is not a numerically demanding task. This is made possible by choosing merit functions depending on two scalar optimization variables at most, keeping the complexity of the problem low and allowing a graphical analysis of the problem. This in turn helps in the assessment of the validity, and usefulness of the proposed optimal approach to sizing.

4. Examples

The aim of the proposed results is firstly that of showing how the design procedures presented above can be profitably used to carry out the preliminary design of small electrically propelled aircraft. This will be demonstrated through two case studies, based on different design requirements. Secondarily, through purpose–built parametric analyses it will be shown what is the behavior of some key design parameters with respect to changes in some of the constraints and mission specifications.

4.1. Specifications

The first example is that of an electric motor–glider. This category is of interest for electric applications at the current technological level, due to the relatively low power and mild propelled–range required. The

second aircraft considered is a more maneuverable, higher–power, faster, lower–range aircraft, intended for over–field hour–building in a semi–acrobatic role.

Tables 2 and 3 show the requirements and polar coefficients respectively for both aircraft, necessary for preparing the respective sizing matrix plots. Most requirements have been set looking at the performance of existing ICE–propelled aircraft in pertinent categories [25, 26].

	Motor–glider	**Acrobatic**
$V_{\text{stall}}^{\text{landing}}$ [kn|m/s]	40|20.6	50|25.7
Take–off run [m]	200	350
Take–off altitude [m]	3000	1500
h^{cruise} [m]	3000	1500
V^{cruise} [kn|m/s]	90|46.3	110|56.6
h^{loiter} [m]	3000	1500
V^{loiter} [m/s]	$0.9\text{V}^{\text{cruise}}$	$0.9\text{V}^{\text{cruise}}$
RC [ft/min|m/s]	400|2.02	2500|12.7
V^{climb} [kn|m/s]	$1.2\text{V}_{\text{stall}}$	$1.2\text{V}_{\text{stall}}$
Power loss exponent ξ [-]	0.98	0.98
η_P [-]	0.85	0.85

Table 2: Specifications for sizing matrix plot for both considered example designs.

The power loss exponent ξ refers to the usual equation modeling the loss of engine performance with altitude [22], yielding $\frac{P(h)}{P_{SL}} = \left(\frac{\rho(h)}{\rho_{SL}}\right)^{\xi}$, where P_{SL} and ρ_{SL} are respectively power and air density at sea level. In the case of electric propulsion, such loss has been hypothesized to be bound mainly to the performance of the propeller, which may be drifting from the design conditions as altitude changes, whereas clearly no loss due to motor conversion efficiency should intervene with altitude. However, due to the relatively small span of working altitudes for the proposed aircraft, this change is not expected to be dramatic, hence justifying the high value assumed for this coefficient.

As the effect on available power due to changing altitude is accounted for separately, propulsive efficiency η_P has been considered constant, neglecting the dependence on speed, as typical in the preliminary stage of the design. This choice can be further justified with low expected changes over the limited speed envelope where the proposed example aircraft are intended to operate, and also with the chance to include variable pitch propellers in a later stage of the design in case this was needed.

The preliminary values for the polar coefficients in Table 3 have been obtained using the procedure presented by Roskam [11] (see Part I). For sizing the parasite share in the total drag, assumptions need to be made concerning the wet surface, based on the weight class of the aircraft, and on the level of refinement of

the aerodynamic design, according to the acceptable limits presented for the corresponding aircraft categories. For both examples, flap deployment has been considered for landing only. Furthermore, parasite drag for the acrobatic example will be increased due to a non–retractable landing gear, typical to this category and not to motor–gliders. The drag–due–to–lift coefficient is determined according to the usual formula $K = \frac{1}{\pi \cdot AR \cdot e}$. Possible values for the Oswald coefficients are suggested by Roskam [11] (see Part I), whereas the aspect ratios have been hypothesized for both examples from existing ICE–propelled aircraft in the respective categories.

	Motor–glider			**Acrobatic**		
Configuration	Clean	Take–off	Landing	Clean	Take–off	Landing
$C_{D,0}$	0.0110	0.0310	0.1010	0.0230	0.0230	0.0930
$C_{L,\max}$	1.5	1.5	2.2	1.5	1.5	2.0
e	0.83	0.83	0.75	0.81	0.81	0.71
AR	30			8		

Table 3: Polar coefficients assumed for both considered example designs.

4.2. Sizing matrix plot

The SMPs for the motor–glider and for the semi–acrobatic aircraft are presented respectively to the left and to the right on Fig. 6. The standard and certification constraints included in the analysis are those for take–off run, climb and landing, whereas from the mission profile further constraints for climb as well as cruise and loiter have been added as shown in the previous methodological section (see Fig. 4 and the corresponding description). For take–off run and standard climb, excerpts from FAR Part 23 for the case of single–engine aircraft have been considered. For take–off they suggest a semi–empirical way to define the power loading necessary for an assigned take–off run based on basic polar coefficients, making use of a very simplistic energy method. For climb, they suggest analyzing the power loading necessary to obtain an assigned RC and climb angle in take–off configuration, and an assigned climb angle in landing configuration (aborted landing).

The curves presented on the SMPs of Fig. 6 have been obtained for assigned values of the polars as in Table 3, and for assigned design values of the lift coefficients for the various configurations, especially for the curves representing take–off, climb and landing, as specified on the plots. Such values are themselves the result of a parametric analysis of the SMP for changing values of the guessed polar values, similarly to Fig. 4. For the sake of clarity, the plots presented in Fig. 6 feature only those curves corresponding to the data presented as specifications in Table 2 and 3 having an impact (or a near impact) on the resulting space of possible solutions.

As specified in the description of the sizing procedure, the choice of the design points, shown as blue stars in the plots, is aimed at increasing wing loading while simultaneously rising power loading. This would reduce

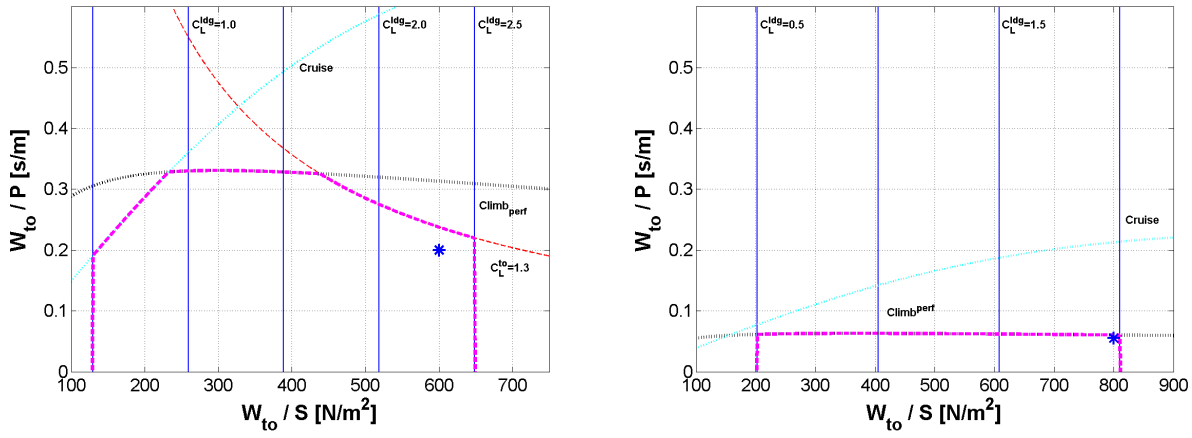

(a) (b)

Figure 6: Sizing matrix plot (SMP). Left: motor–glider. Right: acrobatic. Blue solid lines: landing. Red dashed lines: take–off run. Black dotted lines: climb from mission profile. Cyan dotted line: cruising or loiter speed. Magenta dashed line: envelope. Blue star: chosen design point.

the size of the aircraft and the power required. The two considered scenarios bear rather different results in terms of space of the solutions. The envelope for the motor–glider extends to higher values of power loading, and for increasing values of wing loading it is limited by cruise, by the climb performance requirement from the mission profile, and by take–off distance. On the other hand, the envelope for the acrobatic aircraft is dominated by vertical speed performance coming from the mission profile, limiting the value of power loading to a much lower level with respect to the motor–glider design.

It should be noted that these relative differences between the SMPs for the two designs are clearly in line with the respective roles of the two aircraft categories, and show that the required specifications included in Table 2 are compatible with a realistic solution in terms of wing loading and power loading. Table 4 summarizes the characteristics of the design points for both aircraft.

	Motor–glider	**Acrobatic**
$\frac{W_{to}}{S}$ [N/m^2]	600	800
$\frac{W_{to}}{P}$ [s/m]	0.2	0.055

Table 4: Design values of wing loading and power loading for both considered aircraft.

The design point for the motor–glider is close to the right wing loading limit. This choice rises the requirement on engine power to some extent (the top value for power loading can be attained for wing loading values less than $\frac{W_{to}}{S} = 450$ N/m^2 corresponding to the climb limit of the envelope), but the decrease in wing surface S thanks to a higher wing loading will be advantageous also in terms of drag forces and

power required, besides reducing the size of the aircraft. Furthermore, this choice is in line with respect to similarly designed ICE–aircraft. Differently from the motor–glider case, the design point for the acrobatic aircraft tends to simultaneously maximize both power loading and wing loading.

4.3. Mission profile and weight sizing

Following the work–flow diagram in Fig. 5, once the design values for wing loading and power loading are known from the analysis of the SMP, it is possible to initialize the weight sizing procedure based on the equations for the mission profile, illustrated in the methodological Section 2.2, and the historical regression curve in Eq. 2. The additional performance requirements needed for running the weight computation based on the mission profile are listed in Table 5.

	Motor–glider	**Acrobatic**
R [km]	300	100
T^{loiter} [min]	15	15
W_{pl}/g [kg]	150	100

Table 5: Performance requirements for weight computation based on the analysis of the mission profile for both considered example designs.

The plots reported in Fig. 7 show the result of the weight sizing procedure in terms of W_e and W_{to}. The curves corresponding to the missions of both considered aircraft are reported as blue and red dash–dotted lines respectively for the motor–glider and acrobatic aircraft, whereas the green dashed line represents the regression on historical data. The design points, marked with stars, are on the respective intersections of the mission curves with the regression of historical data. Notwithstanding the differences between the two mission requirements the weight sizing procedure bears remarkably similar results in terms of W_{to} and W_e. Table 6 summarizes the design values for W_{to} and its various components, as well as the power and energy required for flying the intended mission.

The power and motor weight values included in Table 6 show that the motors required for the two designs are very different. The procedure for sizing the electric motor described in Eq. 13 bears a rather high value of W_m for the acrobatic design. Such weight value is not very realistic for a single electric motor. As the aircraft is intended to feature a single propeller – otherwise the sizing and cost evaluation procedures would be somewhat different, and the historical regression data less correct –, a scenario can be envisaged where more motors, with individual weights summing up to the value of W_m, transfer power to the same shaft.

The plots on Fig. 8 show the required energy and power for climb, range and loiter as functions of take–off weight. Similarly to the mission curves presented on Fig. 7, these plots are obtained running the mission profile analysis for different assigned values of W_{to}.

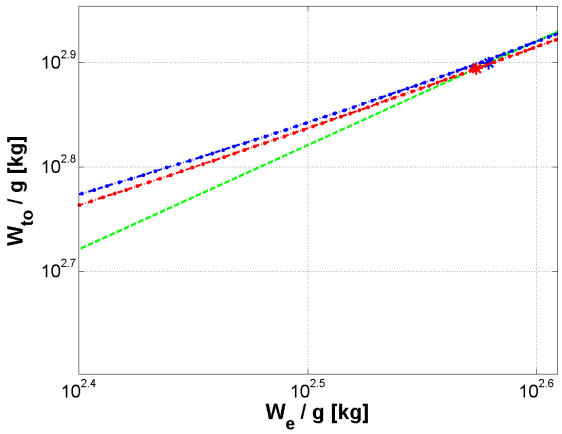

Figure 7: Result of weight sizing for both example aircraft. Blue: mission curve for motor–glider. Red: mission curve for acrobatic aircraft. Green: regression of historical data. Blue star: design point.

	Motor–glider	**Acrobatic**
W_{to}/g [kg]	793	784
W_e/g [kg]	379	375
W_m/g [kg]	23	84
W_{bat}/g [kg]	241	225
W_{pl}/g [kg]	150	100
P_r/η_P [kW]	45.3	162.6
E_r/η_P [MJ]	116.1	108.6

Table 6: Weight components, required power and energy from the integrated sizing procedure for both considered examples.

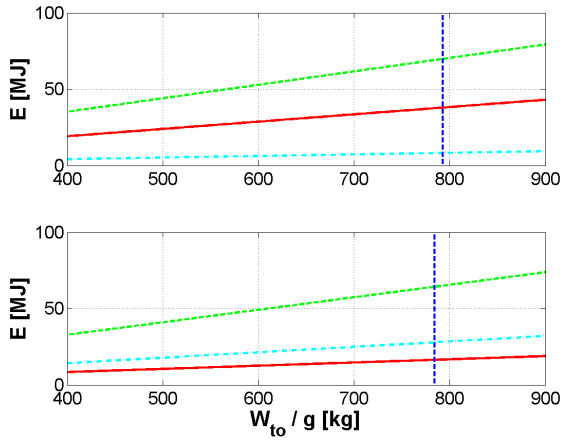

(a) Red solid: climb. Green dashed: cruise. Cyan dash–dotted: loiter. Blue vertical line: design W_{to}.

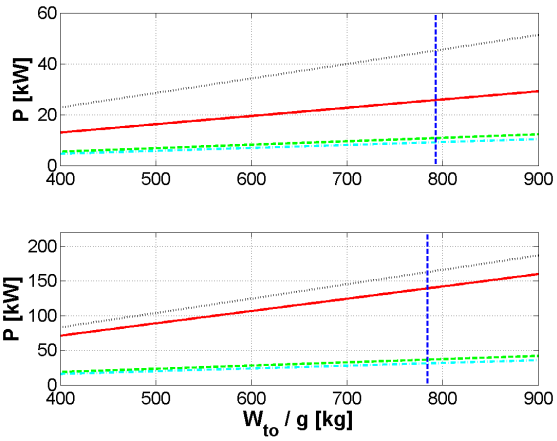

(b) Red solid: climb. Green dashed: cruise. Cyan dash–dotted: loiter. Black dotted: constraint from chosen design point on SMP (climb limitation). Blue vertical line: design W_{to}.

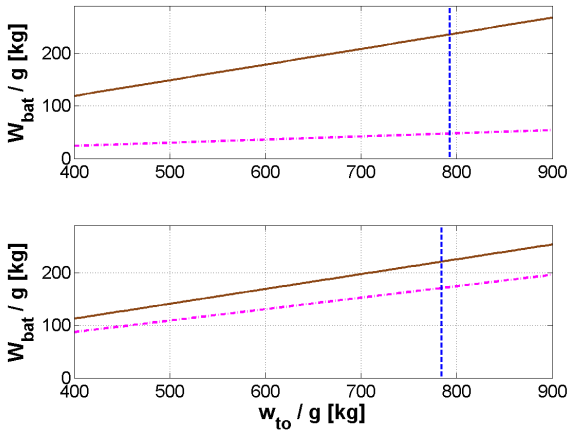

(c) Brown solid: energy requirement. Magenta dash–dotted: power requirement. Blue vertical line: design W_{to}.

Figure 8: Battery energy, power and weight as functions of W_{to}. Top plots: motor–glider. Bottom plots: acrobatic aircraft. Blue vertical line: design W_{to}.

From the energy picture, it can be noticed that the largest share of required energy comes from the cruise phase for both aircraft. On the other hand, it is apparent that the amount of energy pertaining to the various phases of the flight is different for the two designs, the climb phase being particularly requiring for the motor–glider, due to its longer duration in the profile of that aircraft because of the higher cruising altitude and lower required rate of climb. As can be noticed also from Table 6, the overall required energy is comparable for the two designs.

Concerning power, the plots in Fig. 8 present the values pertaining to each phase of the mission, as well as the constraint coming from the design power loading from the SMP. The quality of the results for both aircraft is very similar, with the climb requirement being by far the most stringent of those from the mission profile, and also in absolute terms – i.e. considering all constraints – as can be noticed also from the respective SMPs. The choice of the design SMP leaves a margin with respect to the climb requirement from the mission profile. Contrarily to energy, required power is very different for the two aircraft.

From the plot of the battery weight corresponding to varying values of take–off weight in Fig. 8 it can be noticed that the most stringent requirement on batteries for both designs comes from energy and not from power, even though the acrobatic design requires much more power and the two requirements come very close to one another in this case. The prevalence of the energy requirement is mainly due to the relatively low energy–to–mass density e_{av} of current Li–ion batteries, whereas the corresponding power performance seems to be currently somewhat less critical. It cannot be excluded that further technological developments may change the picture, but as specified at the beginning of the paper, this work is focused on the applicability of the presented methodology to currently feasible designs.

4.4. Quality of the design solution

The quality of the selected solution can be analyzed by introducing some metrics bound to quantities characterizing the design solution and studying the effect on such metrics obtained when changing the design point in terms of power loading and wing loading. The first interesting metrics are take–off weight and its components. In Fig. 9 the behavior of take–off (left) and battery (right) weights is shown for the motor–glider (top row) and the acrobatic aircraft (bottom row). The diagrams are contour plots of W_{to} and W_{bat} obtained running the central block of the procedure in Fig. 5 for various choices of power loading and wing loading.

Figure 9 supports the choice of the design condition to the top–right corner of the envelope, corresponding to lower take–off and battery weights. On the other hand, it can be noticed that for both aircraft the same weight results can be obtained for various choices of wing and power loading, i.e. for every point along a line corresponding to an assigned performance level. Furthermore, in a relatively large area of the envelope around the selected design points, the gradient of the weight solution is not very intense, showing that the area of choice of the design point is more relevant than the exact value of wing and power loading.

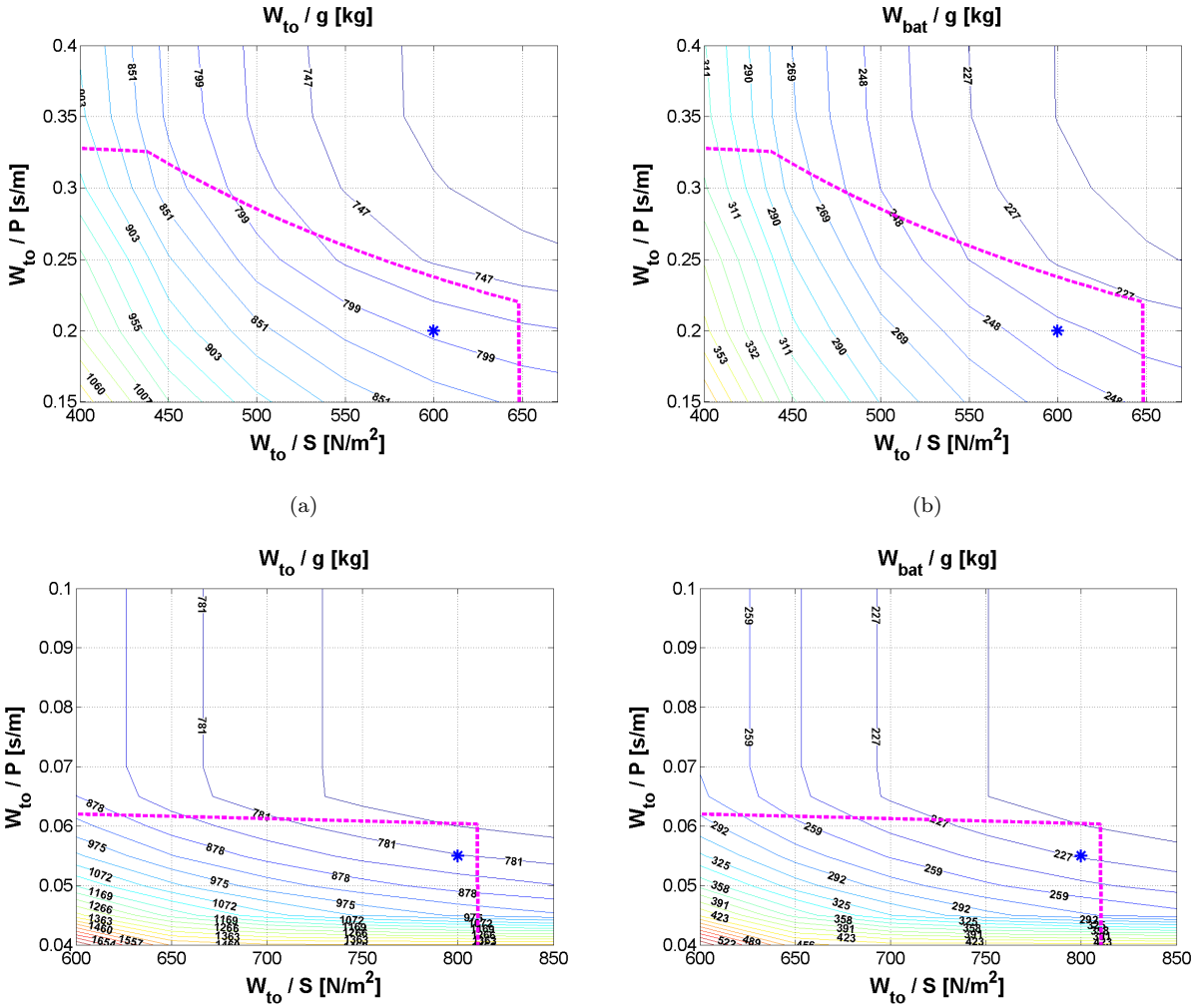

(a) (b)

(c) (d)

Figure 9: Effect of power loading and wing loading on W_{to} (left) and W_{bat} (right). Top row: motor–glider. Bottom row: acrobatic aircraft. Magenta dashed line: SMP envelope. Blue star: design point.

An often important quantity for the design is cost, which can be hypothesized to be proportional to take–off weight and battery weight (Eq. 15 and 16) [24]. The dependence of battery cost on battery weight expressed by Eq. 16 calls for the knowledge of the required power–to–energy ratio of the battery. Figure 10 shows the total value of cost, defined as $C_{AC} + C_{\text{bat}}$, as a function of wing loading and power loading. The resemblance with the behavior of take–off weight is apparent, due to the fact the the cost of the battery is a low fraction of the cost of the aircraft for the considered designs.

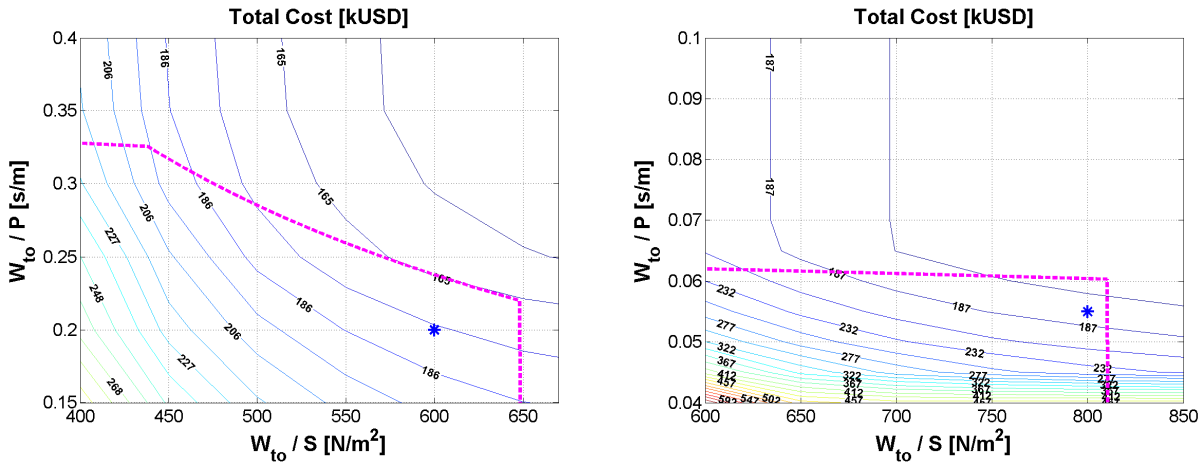

(a) (b)

Figure 10: Effect of power loading and wing loading on total cost. Left: motor–glider. Right: acrobatic aircraft. Magenta dashed line: SMP envelope. Blue star: design point.

It should be noted that the scale of the plots for the two proposed aircraft both in Fig. 9 and 10 is largely different. The area of the respective envelopes is henceforth rather different in absolute terms. Due to the flatness of the plotted functions over the SMP envelopes, this indicates that albeit a similar cost is encountered over the full span of the envelope in absolute terms for both aircraft, this corresponds to many different choices of wing and power loading for the motor–glider and to comparatively less feasible design points in the case of the acrobatic aircraft.

Further information about the quality of the solution come from a parameterized analysis where weight and its components are kept constant to the obtained design values, and some required performance of interest is changed. Figure 11 shows the result of such analysis for the case of the motor–glider, considering range (left) and cruising speed (right) as changing performance parameters. Once again, these result show that a change in the requirements aimed at increasing range or cruising speed would drive the solution towards higher wing and power loading. Even considering these metrics, it is possible to say that the top–right part of the envelope is the most attractive.

The most relevant information which can be obtained from Fig. 11 with respect to the next analysis is

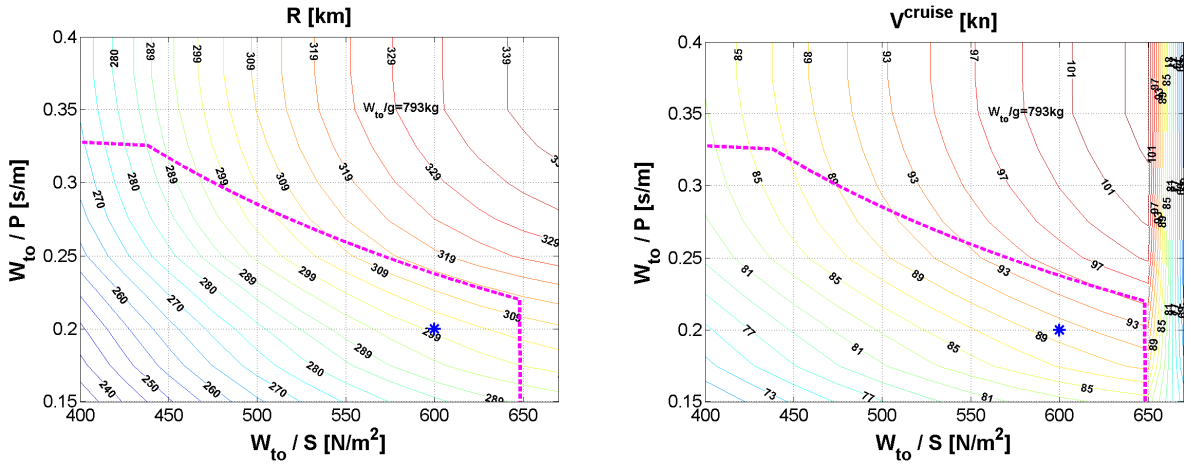

(a) (b)

Figure 11: Effect of power loading and wing loading on range R (left) and V^{cruise} (right) for the case of the motor–glider, for fixed W_{to} as in Table 6. Magenta dashed line: SMP envelope. Blue star: design point.

the fact that both range and cruising speed show a gradient of relevant intensity with respect to wing and power loading.

As for the previous analysis (Fig. 9 and 10), similar results can be obtained for the acrobatic aircraft with respect to range and vertical speed.

4.5. Optimal design

After having highlighted the degree of mutual dependency of the design parameters, it makes sense to study the behavior of the cost functions presented in Eq. 17 and 18 to the aim of understanding whether it is possible to check the level of optimality of the selected design point with respect to a more comprehensive variable, in the form of a merit function depending on more measures of performance. The analysis presented here has been based on the merit functions J^{tour} and J^{acro}, which can be expressed as functions of the two couples of parameters (W_{to}, R) and (W_{to}, RC) respectively, thus allowing showing their behavior through usual contour plots and visually checking it.

The value assumed by J^{tour} for the case of the motor–glider can be seen to the left of Fig. 12, whereas the overall cost for the same design can be seen on the right plot. These quantities have been evaluated for the selected value of wing loading and power loading for the motor glider, hence all solutions here correspond to a feasible point from the viewpoint of the constraints included in the SMP. The black line represents the locus of the solutions for which the equality constraint constituted by the regression on historical data W_{to} vs. W_e in Eq. 2 has been satisfied.

As far as the optimal problem in Eq. 19 is considered, where the historical regression Eq. 2 is imposed as

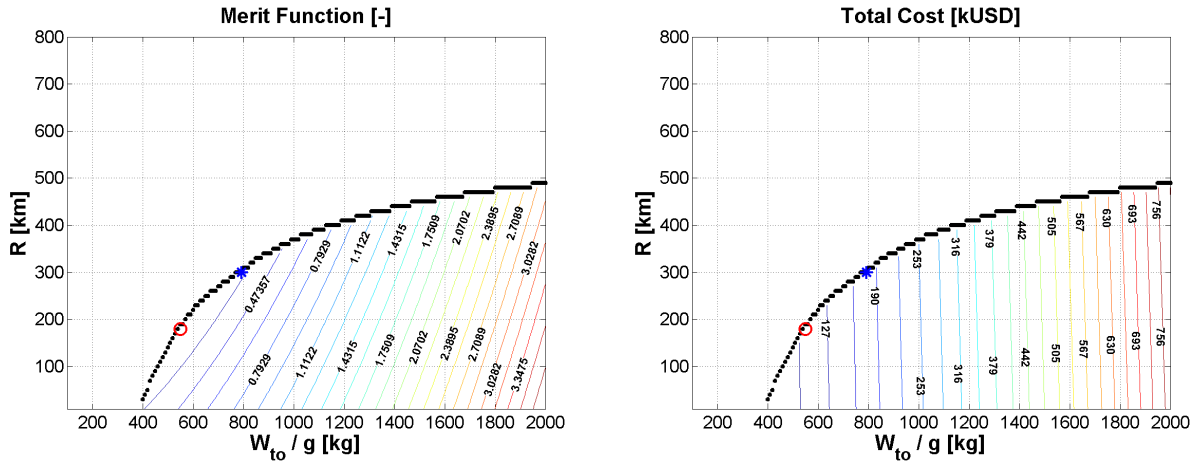

(a) (b)

Figure 12: Merit function J^{tour} (left) and cost (right) as functions of W_{to} and R for the case of the motor–glider. Black dotted line: W_{to} vs. W_e historical regression. Blue star: design point. Red circle: optimum point.

an equality constraint, the black line is the actual space of the solutions of the optimal design problem. For this reason, it is also clear that the solution computed previously by applying the integrated design procedure and represented by the blue star in Fig. 12 should (and does) lie on the black envelope line. In order to get a wider picture of how the design solution would change in case the historical regression constraint were turned into an inequality constraint, stating from Eq. 2 that $\log(W_e) \geq \frac{1}{B}\left(\log(W_{to}) - A\right)$, the plots in Fig. 12 are extended considering those cases for which the empty weight corresponding to a given take–off weight were greater than what is obtained from the historical regression. For this extended space of solutions the limit line is represented by the same black line described above. Conditions for which W_e is lower than what is defined by Eq. 2 for an assigned W_{to} are not considered, on the basis of their lower safety – they would require an excessively lightweight construction, with respect to the lightly powered aircraft included in the database for which the ratio of structural and power–plant weight to W_{to} is already a critical issue.

In the actual computation of the merit function, both range and cost weights q_C and q_R in the function are unitary, so as to obtain a similar share of both components in the overall value of the function. As can be seen to the left of Fig. 12, the value of the merit function tends to decrease for lower values of W_{to}, and for values of R between 100 to 400 km for decreasing W_{to}. A same level of optimality can be obtained for a lower weight and a higher range or viceversa. From the cost plot to the right of Fig. 12, again it can be noticed that this quantity increases mainly with W_{to}, whereas it shows little sensitivity to R. This is due to the fact that the cost of the aircraft excluding batteries, which is bound to W_{to}, is by far the highest fraction of the overall cost.

The position of the design solution, selected independently of the optimal analysis on J^{tour} (i.e. in the

previous paragraphs), is shown as a blue star on the plots of Fig. 12. Considering the adopted setup, metrics and tuning of the optimal problem it can be said that the solution previously selected with the integrated procedure for the motor–glider is not optimal, yet it is not far from the optimum. The position corresponding to the optimum is marked with a red circle. If range is turned into a variable of the design problem, i.e. a design specification that it is possible to tune where necessary, then it will be possible to obtain a cost–range–optimal design solution – in other words, if R is a tunable requirement, it can be chosen to obtain a design solution which optimizes simultaneously cost and range, according to the definition of the adopted cost function J^{tour}, graphically pushing the blue star to the position of the red circle.

Qualitatively similar remarks concern payload weight W_{pl}, which is a relevant design specification that may be considered as a tunable parameter for steering the solution towards an optimum. Considering the plot in Fig. 13, the black envelope line corresponds to the $W_{pl}/g = 150$ kg previously assigned as a design constraint. As already pointed, going down vertically from this line on the same plot corresponds to violating the equality constraint represented by the historical regression W_{to} vs. W_e in Eq. 2. For each W_{to} the difference between the value of W_e obtained from historical data and that computed from the mission profile (i.e. from the top sub–procedure in the central block of the work–flow diagram in Fig. 5) can be interpreted as a change to the weight of transported payload. A contour plot of the so–obtained W_{pl} for every condition on the plane R vs. W_{to} is presented in Fig. 13, under the same hypotheses on the values of W_{to} of interest considered for Fig. 12, again for the case of the motor–glider. Considering a fixed W_{to} it can be noticed that a decrease in range R can be converted into an increase in payload weight W_{pl}. This is true especially for higher values of the overall weight W_{to}, whereas for smaller values, possibly more typical to the considered aircraft category, the advantage may be lower, as can be noticed by the lower gradient of the contoured surface with respect to range in the leftmost area of the considered space of solutions.

A similar analysis can be carried out for the acrobatic example, considering in this case the merit function J^{acro}. Being based on cost and RC, this measure is more meaningful for this kind of aircraft. The following results have been obtained with unitary optimization weights q_C and q_{RC}. In Fig. 14 once again the black line represents the locus of the design solutions satisfying the equality constraint on W_{to} and W_e obtained from the regression curve of historical data. As for the previous case, the result of the integrated design procedure (blue star on the plots) turns out to be not optimal under the selected metrics, i.e. it is not cost–rate–of–climb–optimal, but also in this case it is not far from the optimum, which can be found for nearly the same W_{to} but for an RC increased by about 500 ft/min – see the red circle marking the optimum on the plots of Fig. 14. Total cost is once again dominated by the aircraft cost excluding batteries. For this reason, the contour lines on the corresponding plot to the right are almost vertical, highlighting the fact that according to this cost model the RC performance has not a great influence on total cost. It has indeed an effect on the weight and hence cost of the batteries, whose share in the total cost is however limited for aircraft in this

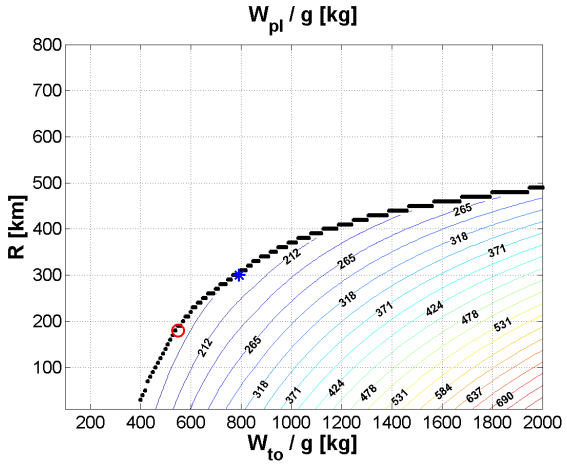

Figure 13: Payload as a function of W_{to} and R for the case of the motor–glider. Black dotted line: W_{to} vs. W_e historical regression. Blue star: design point. Red circle: optimum point.

weight class.

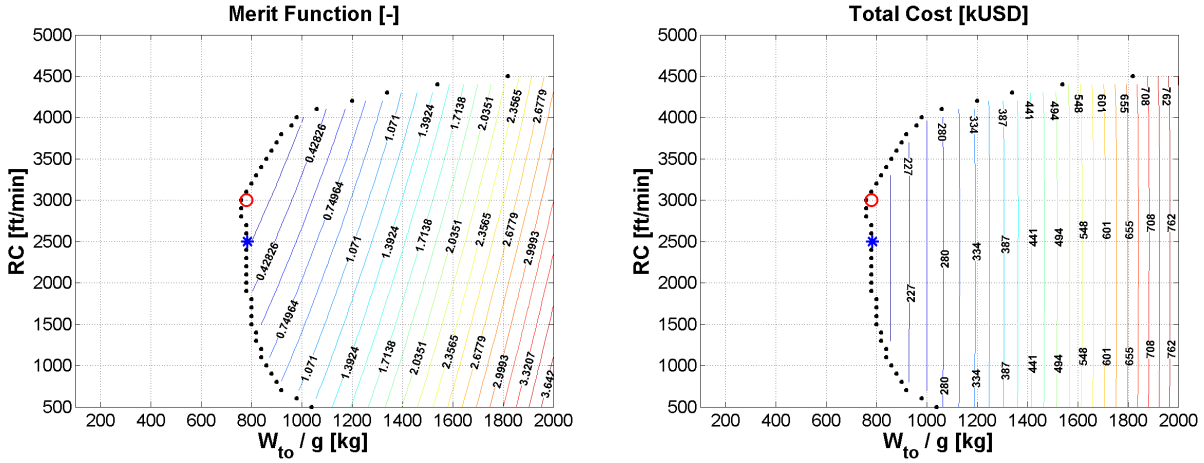

(a) (b)

Figure 14: Merit function J^{acro} (left) and cost (right) as functions of W_{to} and R for the case of the acrobatic aircraft. Black dotted line: W_{to} vs. W_e historical regression. Blue star: design point. Red circle: optimum point.

Similarly to the motor–glider case, by changing the values of one of the design parameters, it will be possible to steer the design point towards the optimum. Looking at the plot to the left of Fig. 14, considering to allow a change in the requirement on RC, the position of the actual optimum (red circle) can be reached by pushing RC to a higher value than the one corresponding to the design solution previously adopted (blue star), while keeping on the black envelope line representing the satisfaction of historical constraints.

The analysis of payload (Fig. 15) bears results qualitatively similar to those previously obtained for

the motor–glider, showing that an increase in W_{to} for the level of RC of the solution selected through the integrated analysis, graphically marked with a blue star, can be translated into a rapidly increasing payload. This is not the case for a RC in a range above 4000 ft/min, for which the gradient of W_{pl} with W_{to} is not so high as for lower RC values.

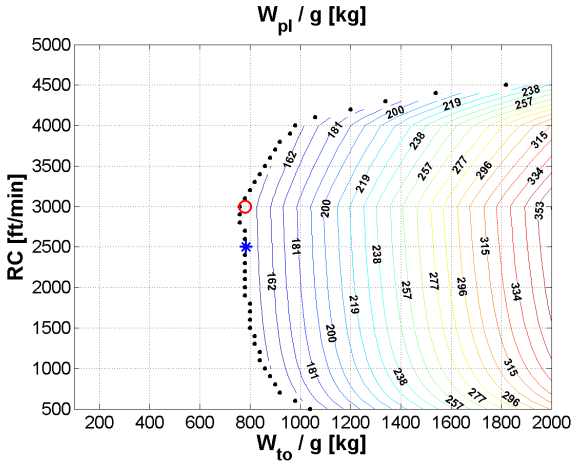

Figure 15: Payload as a function of W_{to} and R for the case of acrobatic aircraft. Black dotted line: W_{to} vs. W_e historical regression. Blue star: design point. Red circle: optimum point.

5. Conclusions

The present paper faces the need to establish a standard procedure for the preliminary sizing of electric aircraft. Starting from the well–known design methods based on the analysis of the sizing matrix plot, and on weight sizing resulting from the simultaneous analysis of the mission profile and of historical data – both tools typically used in the case of ICE–propelled aircraft –, a new integrated procedure mixing both design tools – SMP on one hand, and analysis of historical data and mission profile on the other – is introduced for the specific case of electrically powered aircraft.

The core of the sizing method is a new definition of the partial weights summing up to give the take–off weight, in turn allowing to study the mission profile without making use of fuel fractions, which are meaningless quantities for an electrically powered aircraft. The new procedure couples the results of the analysis of the sizing matrix plot with the weight sizing procedure, yielding an integrated sizing procedure.

Furthermore, the paper shows that an approach to weight sizing based on statistical analysis of historical data can be still exploited also for electrically propelled aircraft, due to the good correlation between data pertaining to existing aircraft. Statistics are used not only for linking take–off and empty weight values as mostly usual for ICE–propelled aircraft, but also for relating power and weight of electric motors, and again in the battery sizing phase, when it is necessary to translate a power or energy requirement into the

corresponding weight of batteries. The database extends to a rather restricted aircraft category, implicitly limiting the analysis to smaller aircraft. This has been accepted as a limit, with the advantage of making the results of the analysis safer and attainable with current technologies – i.e. free from futuristic technological projections.

In order to show a possible way to fully exploit the proposed procedure, which is straightforward and computationally light, some computational–intensive analysis have been proposed, where the design is optimized by preliminarily defining a cost function including cost and key performance of the aircraft. Cost is accounted for by considering cost models specific to small aircraft and to batteries at the current level of technology.

A complete preliminary sizing is illustrated for two possible aircraft in the weight category of the considered database but with different mission requirements, showing that standard analyses also typical to ICE–propelled aircraft, albeit modified to encompass the specific procedures presented in this paper, can be carried out bearing realistic results. The reasonable results obtained with such analyses, based on battery data pertaining to existing batteries and specifically not to futuristic designs, tend to confirm the validity of the design procedure.

A limit of the proposed procedure is that of considering a relatively small database of aircraft, making the exploration of aircraft in other weight categories more difficult. Scaling problems connected with the preliminary design of electrically powered aircraft will be the subject of a research work to follow.

Declaration of conflicting interests

The Authors declare that there is no conflict of interest.

Funding

This research received no specific grant from any funding agency in the public, commercial, or not–for–profit sectors.

References

[1] W. Cao, B.C. Mecrow, G.J. Atkinson, J.W. Bennett, and D.J. Atkinson, Overview of Electric Motor Technologies Used for More Electric Aircraft (MEA), IEEE Transaction on Industrial Electronics, 59(2012) 3523–3531.

[2] B. Bilgin and A. Emadi, Electric Motors in Electrified Transportation, IEEE Power Electronics Magazine, 1(2014) 10–17.

[3] R.H. Lyon, Machinery Noise and Diagnostics, Butterworths, First Edition, 1987.

[4] K. Ozawa, Lithium–ion Rechargeable Batteries, Wiley–VCH, First Edition, 2009.

[5] G. Pistoia, Electric and Hybrid Vehicles, Elsevier, First Edition, 2010.

[6] C. Pornet, S. Kaiser, A.T. Isikveren, and M. Hornung, Integrated Fuel–Battery Hybrid for a Narrow–Body Sized Transport Aircraft, Aircraft Engineering and Aerospace Technology: An International Journal, 86(2014) 568–574.

[7] C. Pornet, C. Gologan, P.C. Vratny, A. Seitz, O. Schmitz, A.T. Isikveren, and M. Hornung, Methodology for Sizing and Performance Assessment of Hybrid Energy Aircraft, Journal of Aircraft, 52(2015) 341–352.

[8] T.P. Choi, D.S. Soban, and D.N. Mavris, Creation of a Design Framework for All–Electric Aircraft Propulsion Architectures, in: 3rd International Energy Conversion Engineering Conference, San Francisco, CA, August 15–18, 2005.

[9] S.M. Batill, M.A. Stelmack, and X.Q. Yu, Multidisciplinary Design Optimization of an Electric–Powered Unmanned Air Vehicle, Aircraft Design, 2(1999) 1–18.

[10] B.A. Moffitt, T.H. Bradley, D.E. Parekh, and D.N. Mavris, Design and Performance Validation of a Fuel Cell Unmanned Aerial Vehicle, in: 4th AIAA Aerospace Sciences Meeting and Exhibit, Reno, NV, January 9–12, 2006.

[11] J. Roskam, Airplane Design, Part I–VII, DARcorporation, Second Edition, 2003.

[12] D.P. Raymer, Aircraft Design: A Conceptual Approach, AIAA Education Series, Fifth Edition, 2012.

[13] Electravia, ZA Aérodrome, 04200 Vaumeilh, France. Website: `www.electravia.fr`.

[14] JSC Sportine Aviacija ir Ko, Pociunai LT–59327, Prienai, Lithuania. Website: `www.lak.lt`.

[15] Lange Aviation GmbH., Brüsseler Straße 30, D–66482 Zweibrücken, Germany. Website: `www.lange-aviation.com`.

[16] Pipistrel d.o.o. Ajdovščina, Goriska Cesta 50a, SI–5270 Ajdovščina, Slovenia. Website: `www.pipistrel.si`.

[17] UAV Factory USA LLC., 50 South Buckhout Street, Irvington, NY 10533, USA. Website: `www.uavfactory.com`.

[18] Yuneec Americas (USA), 5555 Ontario Mills Parkway, Ontario, CA 91764, USA. Website: `www.yuneec.com`.

[19] Alisport srl., via Confalonieri 22, 23894 Cremella (LC), Italy. Website: `www.alisport.com`.

[20] M. Hagen, S. Dörfler, P. Fanz, T. Berger, R. Speck, J. Tübke, H. Althues, M.J. Hoffmann, C. Scherr, and S. Kaskel, Development and Costs Calculation of Lithium-Sulfur Cells with High Sulfur Load and Binder Free Electrodes, Journal of Power Sources, 224(2013) 260–268.

[21] M. Hagen, D. Hanselmann, K. Ahlbrecht, R. Maça, D. Gerber, and J. Tübke, Lithium-Sulfur Cells: The Gap between the State–of–the–Art and the Requirements for High Energy Battery Cells, Advanced Energy Materials, 5(2015).

[22] G.J.J. Ruijgrok, Elements of Airplane Performance, Delft University Press, 2009.

[23] E.A. Estrada Rodas, J.H. Lewe, and D. Mavris, Feasibility Focused Design of Electric On–Demand Aircraft Concepts, in: 14th AIAA Aviation Technology, Integration, and Operations Conference, Atlanta, GA, June 16–20, 2014.

[24] S. Gudmundsson, General Aviation Aircraft Design, Butterworth–Heinemann, First Edition, 2013.

[25] R. Simpson, Airlife's World Aircraft, Crowood Press, 2001.

[26] L.R. Jenkinson and J.F. Marchman III, Aircraft Design Projects, Butterworth–Heinemann, First Edition, 2003.

[27] M.A. Kromer and J.B. Heywood, Electric Powertrains: Opportunities and Challenges in the U.S. Light–Duty Vehicle Fleet, Technical Report LFEE2007–03RP, Sloan Automotive Laboratory, Massachusetts Institute of Technology, Cambridge, MA, 2007.

[28] C. Pornet and A.T. Isikveren, Conceptual Design of Hybrid–Electric Transport Aircraft, Progress in Aerospace Sciences, 79(2015) 114–135.

[29] L.W. Traub, Range and Endurance Estimates for Battery–Powered Aircraft, Journal of Aircraft, 48(2011) 703–707.